Reaction measurements and analyses for $^3He + ^4He$ at 15.95 MeV (c.m.)*

J. A. Koepke and Ronald E. Brown†
John H. Williams Laboratory of Nuclear Physics, University of Minnesota, Minneapolis, Minnesota 55455
(Received 31 March 1977)

A study has been made of the proton and α-particle yields from the 28-MeV (lab) bombardment of ^4He by ^3He. From these measurements a total reaction cross section σ_R of 433 ± 10 mb was deduced. A reaction-model analysis of the α-particle continuum revealed a significant contribution from the sequential reaction $^3He + ^4He \rightarrow ^6Li(2.18) + p \rightarrow \alpha + d + p$ in which the breakup of the excited ^6Li nucleus is nearly isotropic in its rest system. A phase-shift study was performed for $^3He + ^4He$ elastic scattering at this energy using our σ_R value as a constraint. A pronounced odd-even dependence of the real parts of the phase shifts on the orbital angular momentum was found. The results of this work are compared with other experiments, optical-model and phase-shift analyses, and resonating-group calculations.

[NUCLEAR REACTIONS $^4He(^3He,p)$, $(^3He,\alpha)$, $E=28.00$ MeV; measured $\sigma(E_p,\theta)$, $\sigma(E_\alpha,\theta)$; deduced σ_R. α-continuum analysis. Phase-shift analysis. Resonating-group comparison.]

I. INTRODUCTION

Attempts to extract information from elastic-scattering data on properties of the interaction between two nuclei often yield ambiguities in the extracted values of some of the parameters of the model or theory being used. Because absorption processes affect the elastic channel and because the total reaction cross section σ_R is an overall measure of these processes, such ambiguities sometimes can be reduced by imposing the constraint that the model or theory yield σ_R values in agreement with experiment. The principal motivation for making σ_R measurements generally has been to use the results in such applications. For example, in extracting phase shifts from elastic-scattering data one can use the results of σ_R measurements to restrict the allowed range of values of the imaginary parts of the phase shifts. Also, in some optical-model analyses it has been found that measured σ_R values can be used to impose useful restrictions on the parameters of the imaginary potential.[1,2] In addition, the inclusion of phenomenological imaginary potentials in resonating-group calculations[3] for light systems has made it useful to have σ_R measurements for such systems. Specifically, for the $^3He + ^4He$ system of interest here, previous work includes phase-shift analyses,[4-9] optical-model studies,[10,11] and resonating-group calculations.[12-18]

In the present experiment we measured the $^3He + ^4He$ total reaction cross section σ_R by summing appropriate partial reaction cross sections. Such a method involves measuring angular distributions and generally is more tedious and time consuming than the anticoincidence beam-attenuation method.[1,2,19-23] However, at low energies the beam-attenuation method usually becomes inaccurate due to large elastic-scattering corrections, and furthermore the summation technique may become easier to employ at low energies where fewer reaction channels are open. Thus, the two methods tend to complement each other. Of course, the summation method yields information on partial reaction cross sections as well as on σ_R. Recently the beam-attenuation method has been used[23] to measure σ_R for the light systems $p + ^3He$ and $p + ^4He$, and some work has been carried out using this summation method to measure σ_R for the systems $d + d$ (Ref. 24) and $^3He + ^3He$ (Ref. 25).

Although the primary purpose of the present work was to measure the total reaction cross section σ_R, information was also obtained on the mechanisms involved in the $^3He + ^4He$ reaction by carrying out a least-χ^2 fit of a simple reaction model to our ^4He-continuum data. There were principally two reasons for performing this model analysis of the continuum. First, it was desired to have some theoretical guide for the data extrapolations necessary to extract σ_R. Second, in view of the fact that the work of Ref. 26 at higher energies had yielded ^4He-continuum structure which was interpreted as having been produced by sequential decay through $^6Li^*$ (2.18 MeV), it was desired to determine whether or not such two-step decay also occurs with significant probability at our energy. The fit was good enough to accomplish both objectives, and is described below in Sec. V.

One use to which we put our measured value of σ_R was as a constraint in a phase-shift analysis for $^3He + ^4He$ scattering at 15.95 MeV (c.m.). This is described below in Sec. VI, and had as one of its main purposes the investigation of whether or

not a phase-shift solution exists for which the phases have values near those of the resonating-group results of Ref. 18. Finally, in Sec. VII our value for σ_R is included in a discussion of the general trend of σ_R with energy exhibited by results from other phase-shift analyses,[4,9] optical model studies,[10,11] and resonating-group calculations which included a phenomenological imaginary potential.[18]

II. MEASUREMENT SCHEME

The general method of measuring a total reaction cross section σ_R by detecting a sufficient number of reaction-product species often allows several variations in the measurement scheme, depending on the specific reactions possible at a particular bombarding energy. For example, for the ^{3}He+^{4}He system at $E_{c.m.}$ = 15.95 MeV one variant of this method arises from considering two classes of open reaction channels: those which produce continuum ^{4}He particles, and those which do not. Two ^{4}He-producing reactions are the simultaneous breakup of the incident ^{3}He particle into two particles

$$^3\mathrm{He}+{}^4\mathrm{He}\rightarrow{}^4\mathrm{He}+p+d, \tag{1}$$

and into three particles

$$^3\mathrm{He}+{}^4\mathrm{He}\rightarrow{}^4\mathrm{He}+p+p+n. \tag{2}$$

Several two-step sequential processes[26] also terminate with the same final state particles given in Eqs. (1) and (2). An example of a two-step process which terminates in the final state particles given in Eq. (1) is

$$^3\mathrm{He}+{}^4\mathrm{He}\rightarrow{}^6\mathrm{Li}^*+p \quad\searrow\quad {}^4\mathrm{He}+d, \tag{3}$$

and an example for the final state particles given in Eq. (2) is

$$^3\mathrm{He}+{}^4\mathrm{He}\rightarrow{}^6\mathrm{Be}+n \quad\searrow\quad {}^4\mathrm{He}+p+p. \tag{4}$$

The reactions which do not produce ^{4}He particles are as follows:

$$^3\mathrm{He}+{}^4\mathrm{He}\rightarrow{}^7\mathrm{Be}+\gamma, \tag{5}$$

$$^3\mathrm{He}+{}^4\mathrm{He}\rightarrow p+{}^6\mathrm{Li}, \tag{6}$$

$$^3\mathrm{He}+{}^4\mathrm{He}\rightarrow{}^6\mathrm{Li}^*+p \quad\searrow\quad {}^6\mathrm{Li}+\gamma. \tag{7}$$

The cross section for the radiative capture reaction in Eq. (5) is expected[27] to be insignificant compared to the magnitudes of the other processes listed, and therefore, this contribution to the total reaction cross section will be neglected.

All ^{4}He-producing reactions eventually terminate with the final state particles given in Eq. (1) or (2), and in each case only one ^{4}He particle is produced. Therefore, the reaction cross section for this class of reactions, which we shall designate by σ_α, can be measured by counting only ^{4}He particles (excluding elastically scattered recoil ^{4}He particles). Furthermore, the cross sections for the reactions of Eqs. (6) and (7) are easily measured by detecting the nearly monoenergetic protons. The ^{6}Li ground state is stable, and the second excited state decays only by γ emission.[28] All other states of ^{6}Li in our range of excitation (0–12 MeV) decay with overwhelming probability by particle emission.[28] The sum of the cross sections for the formation of the ground and second excited states of ^{6}Li, which we shall designate by σ_p^*, then need only be added to the cross section σ_α for production of continuum ^{4}He particles to obtain the total reaction cross section:

$$\sigma_R=\sigma_\alpha+\sigma_p^*. \tag{8}$$

This equation represents a way in which the total reaction cross section may be measured, and, as mentioned below, represents the method actually used here. However, expressions for the total reaction cross section are also given by

$$\sigma_R=\sigma_n+\sigma_d+\sigma_p^*, \tag{9}$$

or

$$\sigma_R=\tfrac{1}{2}(\sigma_p+\sigma_d+\sigma_p^*), \tag{10}$$

where σ_n, σ_p, and σ_d are the cross sections for production of neutrons, protons, and deuterons, respectively. A detailed deviation of Eqs. (9) and (10) is given in Ref. 29. These equations represent two other possible ways of measuring σ_R. In each of Eqs. (8)–(10) the measurement of σ_p^*, the reaction cross section for the production of ^{6}Li in its ground and second excited states, is required. Equation (10) requires the additional measurement of the cross sections for production of neutrons and deuterons, Eq. (9) requires the additional measurement of the cross sections for the production of protons and deuterons, and Eq. (8) requires only the additional measurement of the cross section for production of continuum ^{4}He particles. Because of its greater simplicity, the scheme represented by Eq. (8) was chosen for the present measurement of σ_R.

III. EXPERIMENT

A. Apparatus

The apparatus used in this experiment has been described in detail in Refs. 29–31 and only a brief description will be given here.

The MP tandem accelerator at the John H. Williams Laboratory of Nuclear Physics produced a ^{3}He beam which was magnetically analyzed and directed through a ^{4}He-filled gas cell situated at the center of a 43-cm-diam scattering chamber. The energy of the incident ^{3}He beam was such that its energy at the center of the gas cell was 28.00 MeV, an energy at which reasonably accurate differential-cross-section measurements exist.[14] The beam was collected in a large Faraday cup having magnetic fields located so as to keep electrons produced in the target from entering the cup and to keep secondary electrons produced in the cup from leaving it. The gas cells were enclosed by 6-μm-thick Kapton foils.[32] The cell used for the ^{4}He continuum measurements had a 3.5-cm-long entrance snout, whereas the cell used for the proton measurements was the unsnouted cell mentioned in Ref. 31. The additional shielding of the beam-entrance foil by the snout helped to reduce background in the energy region of the ^{4}He continuum.

Two detector assemblies were used, each of which employed silicon, surface-barrier detectors which viewed the target gas through a standard, gas-target, collimator assembly. One served as a monitor of the elastic yield at a fixed angle (70°) and had a single detector; the other served to measure, in separate experiments, proton and ^{4}He differential cross sections and had multidetector stacks—one stack for proton detection and another for ^{4}He detection.

The electronic instrumentation consisted of charge-sensitive preamplifiers, linear amplifiers, linear adders, single-channel pulse-height analyzers (SCA), coincidence units, computer interfaced scalers, analog-to-digital converters (ADC), and an on-line computer.

B. Procedure

1. Measurement of proton yield

For this measurement a three-detector, ΔE-E, particle-identification system was used to separate proton events from other charged particle events. The thicknesses of these detectors were, from front to back, 100, 250, and 3000 μm. This arrangement allowed the choice of either a 100-μm ΔE detector with a 3250-μm E detector (middle and back detector signals summed) or a 350-μm ΔE detector (front and middle detector signals summed) with a 3000-μm E detector. The thick (350 μm) ΔE detector arrangement was used for measurements at forward laboratory angles from 15° to 80° and the thin (100 μm) ΔE detector arrangement was used at the more backward laboratory angles from 80° to 130°. Beyond 130° particle identification was not used because there the proton groups of interest did not overlap in energy with other particle types.

The amplified pulses from the ΔE and E detectors were each connected to an SCA and to an ADC. A 0.5-μsec coincidence was required between the two SCA output signals, and the coincidence signal was scaled and served as a gating signal for the ADC system. In this way we readily determined the dead time of the ADC system, which gave the only significant contribution to the total electronic dead time. Particle-type identification was accomplished on line via computer software. A sample proton energy spectrum is shown in Fig. 1.

2. Measurement of ^{4}He-continuum yield

Data on the ^{4}He continuum were obtained by using a two-detector stack consisting of a 27-μm-thick front detector and a 500-μm-thick back detector. If we had employed this stack as a standard ΔE-E particle-indentification system, the lowest energy ^{4}He particle which could have been detected would have been about 6.5 MeV. However, the ^{4}He continuum extends nearly to zero energy, and, because an accurate determination of the total reaction cross section depends on the measurement of a large portion of this continuum, a novel mode of operation of the detector stack was used which allowed the detection of ^{4}He particles of energies down to 1.8 MeV.

In this mode of operation, the signals from the 27- and 500-μm detectors were added, with appropriate gating, to produce an energy spectrum.

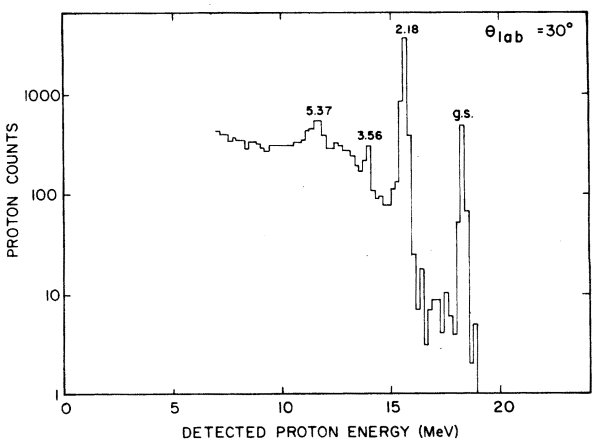

FIG. 1. Proton spectrum at 30° (lab) produced by 28-MeV ^{3}He bombardment of ^{4}He. Prominent peaks correspond to the residual nucleus ^{6}Li being left with the indicated excitation energies (MeV). The spectrum suggests that the broad state at 4.31 MeV is probably formed also.

One of the gating requirements was that no particle event would be accepted unless the particle deposited in at least one of the detectors an energy greater than the deuteron stopping energy in that detector. This corresponds to an energy loss of either 1.7 MeV in the 27-μm detector or 11 MeV in the 500-μm detector. Such an arrangement allowed the rejection of proton and deuteron events of all energies and the acceptance of ^{4}He-continuum events of energies from 1.8 to 23.6 MeV. In addition, ^{6}Li events with energies between 5.6 and 17.5 MeV were eliminated by the further gating requirement that no particle event would be accepted if the particle deposited more energy in the front detector than the ^{4}He stopping energy of 5.5 MeV for that detector. There was no need to arrange the system to reject either tritons or ^{3}He particles because reaction channels which produce tritons are not open at 15.95 MeV (c.m.) and the energy of the elastically scattered ^{3}He particles is always higher than the maximum energy possible for a continuum ^{4}He particle. This system does have an acceptance range of 1.8 to 5.6 MeV for ^{6}Li particles; however, the kinematics and gas-cell energy-loss characteristics of the ^{6}Li particles produced in the reaction of Eq. (6) were such that at only one laboratory angle (22°) was it necessary to subtract the events in a ^{6}Li group from the ^{4}He continuum events. A schematic diagram of the method by which the above gating requirements were imposed is given in Fig. 2. This electronic arrangement allows the data to be corrected for ADC dead time.

The energy scale for the continuum measurements was established by measuring peak positions of the elastically scattered ^{3}He particles and recoil ^{4}He particles and by calculating the energies of these detected particles from kinematic relations and energy loss formulas.

Spectra were obtained at several lab angles by bombarding an evacuated gas cell. These measurements showed that there was no significant contribution from foil scattering to the energy region of the ^{4}He continuum. There was, however, a contribution to this region from those elastically scattered ^{3}He and ^{4}He particles whose energy had been degraded appropriately in the detector collimators. Corrections for this "slit scattering" were made by the extrapolation to low energy of the slit-scattering background appearing in the

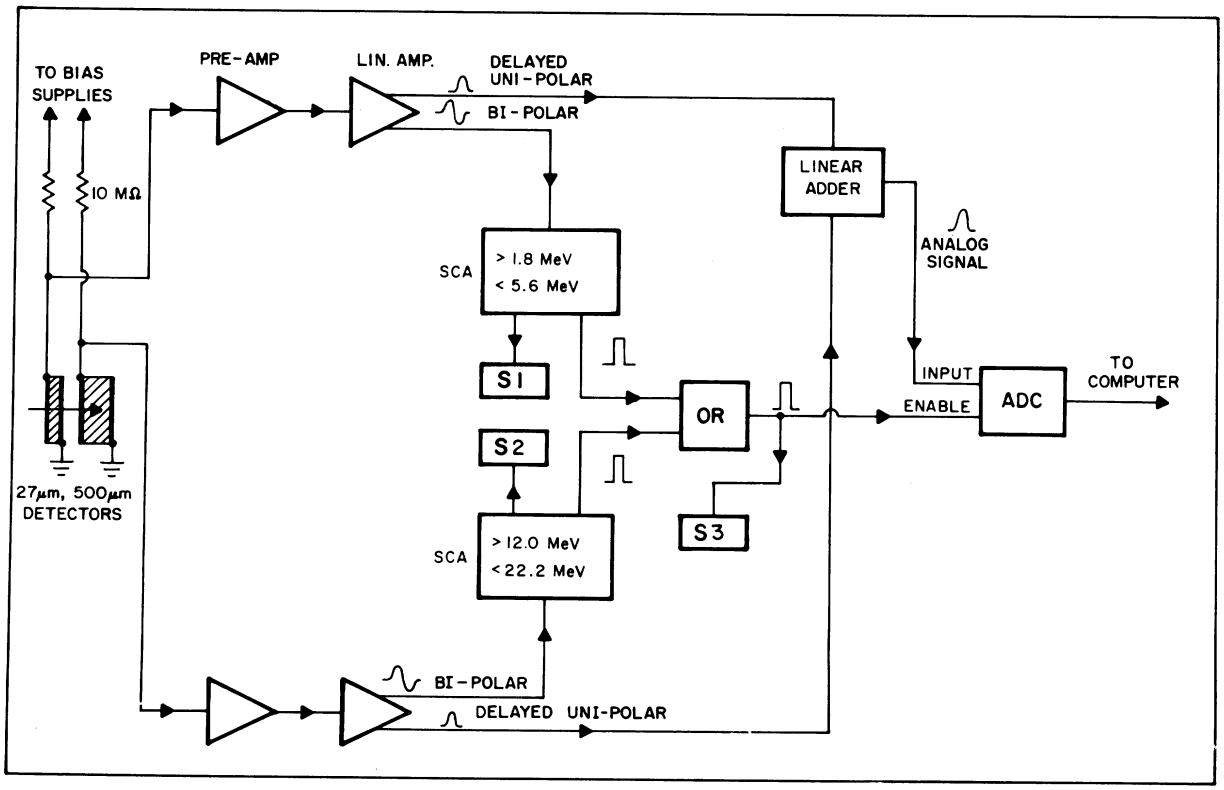

FIG. 2. Electronic arrangement for the measurement of the ^{4}He continuum as described in Sec. III B 2. The units S1, S2, and S3 are scalers. The OR unit produces an output pulse to enable the ADC whenever it receives one or more input pulses.

spectrum at energies above the continuum region. These corrections ranged from 2 to 10% of the measured continuum yield. Several background-subtracted and energy-loss corrected continuum spectra are shown as histograms in Fig. 3.

3. *Other procedures*

The absolute normalization of the entire data-taking system was checked by comparing differential cross sections extracted from the ^{3}He and ^{4}He elastic yields obtained in this experiment with the elastic scattering data at 15.95 MeV (c.m.) of Ref. 14. There was agreement to within 3%, which is quite satisfactory.

The monitor detector was set at an angle of 70° where the ^{3}He differential cross section has a relative maximum. Thus its counting rate was not very sensitive to minor changes in beam direction, and its main purpose was to allow observation of possible drifts in the apparatus for measuring target-gas pressure, target-gas temperature, and integrated beam current.

C. Errors

We assign an error of ±1% to the absolute scale of our measured differential cross sections. Somewhat less than half of this error arises from uncertainties in detection geometry, beam-current integration, and target-gas temperature and pressure. The remainder of the error is assigned to account for a variety of small effects for which corrections were not made to the data. These effects include nuclear reactions of the detected particles with the Si detector material, multiple scattering of the detected particles in the gas-cell foil, and deviations of the true reaction angle from the nominal angle (data were not taken both left and right of the incident-beam direction). Corrections, had they been made, for many of these additional effects would have been angle dependent, and their associated errors then would have been included in the relative error. This more correct procedure would have resulted in only very small changes in the relative errors, and therefore the procedure actually adopted is quite sufficient. The assigned relative errors include effects from counting statistics and uncertainties in background subtraction.

IV. EXPERIMENTAL RESULTS

A. Proton yield

A 30° (lab) proton energy spectrum is shown in Fig. 1. As was mentioned in Sec. II, the production of protons leading to ^{6}Li(g.s., $T=0$) and

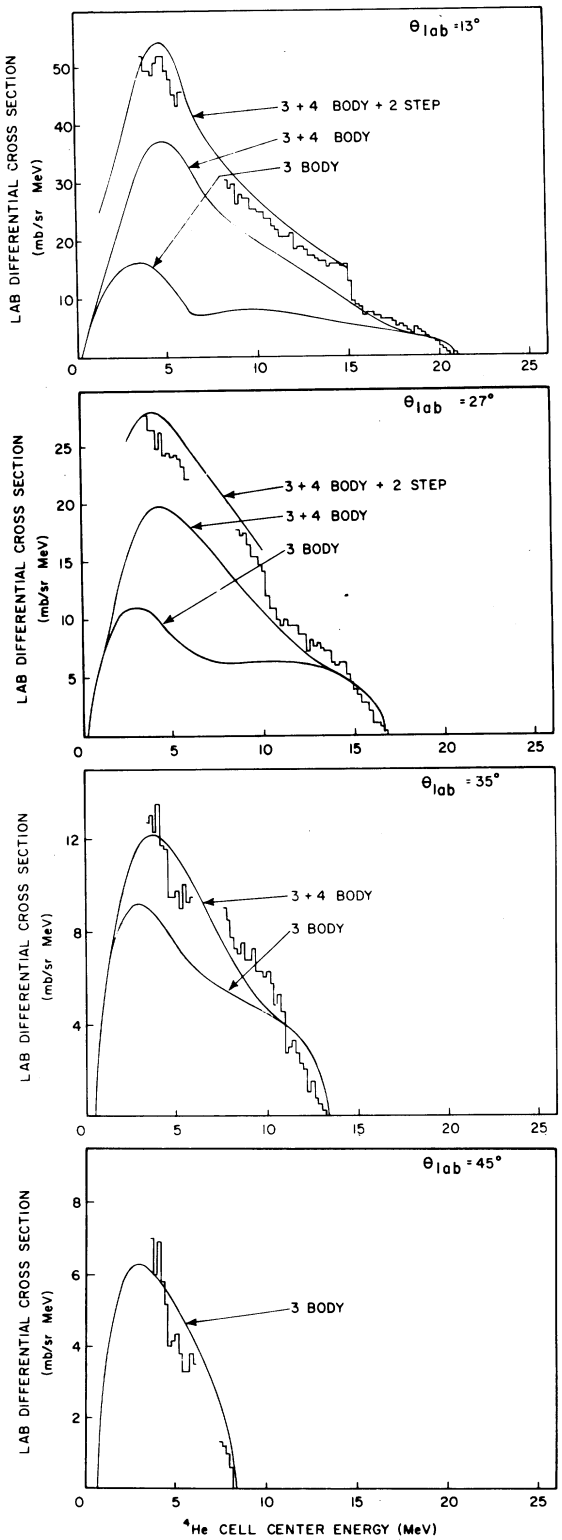

FIG. 3. Selected background-subtracted and energy-loss-corrected ^{4}He-continuum spectra (histograms) at the indicated lab angles θ_{lab} from 28-MeV ^{3}He bombardment of ^{4}He. The energy axis indicates the ^{4}He energy at the center of the gas target.

to $^6Li^*$(3.56 MeV, $T=1$) are of importance in determining the total reaction cross section σ_R, and therefore these differential cross sections were measured. In addition, we measured the differential cross section for production of protons leading to $^6Li^*$(2.18 MeV, $T=0$). It will be seen in Sec. V that these latter data were quite useful in helping to understand the results of the ^4He continuum measurements. These three sets of differential cross sections are plotted in Fig. 4. The points in this figure correspond to the measured data, and the solid curves represent the results of Legendre-polynomial, least-χ^2 fits to the data. Integrated cross sections were extracted from these fits, and the results are 32 ±1 mb for the ground-state reaction and 81 ± 2 mb for the reaction leading to the ^6Li first excited state at 2.18 MeV. The proton peak corresponding to the ^6Li second excited state at 3.56 MeV blended into the background beyond 100°, and because of the resulting lack of data, a reasonable Legendre-polynomial fit was not achieved. A graphical estimate yields an integrated cross section of 3 ± 1 mb, which gives only a small contribution to σ_R.

Our measured differential cross sections for proton production are listed in Table I.

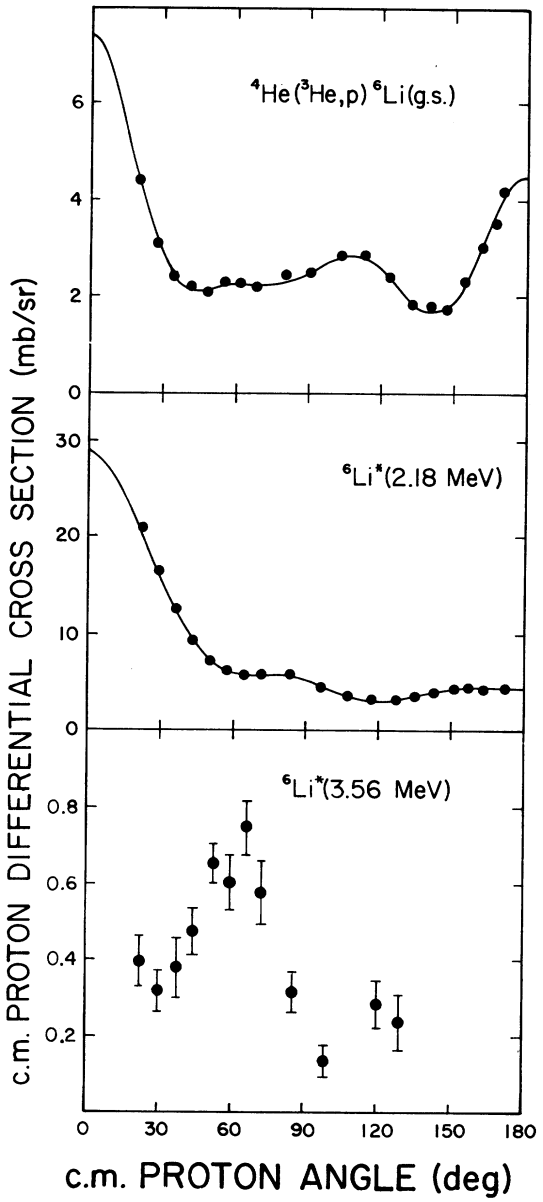

FIG. 4. c.m. differential cross section for $^4He(^3He,p)^6Li$ reactions from 28-MeV ^3He bombardment of ^4He. The data (solid circles) are from Table I. The solid curves show the results of Legendre-polynomial fits.

B. ^4He continuum yield

^4He continuum data were taken at 14 laboratory angles from 13° to 45°. A portion of this data is shown as histograms in Fig. 3. All of the spectra shown have been corrected for gas-cell energy losses and for counts produced by the low-energy tails of the elastic ^3He and ^4He peaks. It will be noticed that the data in a 1-MeV interval about 6 MeV have been deleted. This was done because a dead layer near the front surface of the 500-μm detector caused a distortion of the spectrum in this region. The total number of continuum events in this region was not affected, however, and therefore the contribution of this region to the differential cross section is known.

At each laboratory angle the energy-integrated cross section for production of ^4He continuum particles was calculated. To do this it was necessary to include an estimate of the contribution from the low-energy region of the spectrum where no data were available. These estimates were obtained by assuming that the shape of the low-energy part of the spectrum was given by a straight line segment drawn between the origin and the lowest energy data point. The uncertainty in each estimate was taken to be $\frac{1}{3}$ of that estimate. We note here that the continuum-fitting method described below in Sec. V gave a low-energy contribution close to that obtained from our simple linear extrapolation. The energy-integrated differential cross sections obtained with this procedure were multiplied by the sine of the lab angle and then graphed as points with error bars in Fig. 5.

Integration over angle of the data in Fig. 5 yields a value of 318 ± 6 mb for the contribution from the ^4He continuum in the angular region between 13° and 45°. An estimate of 70 ± 5 mb for the integrated cross section from the 0° to 13° region was obtained by assuming that the angular dependence in this region is given by a straight line segment

TABLE I. c.m. differential cross sections $\sigma_{c.m.}$ vs lab angle θ_{lab} at a lab energy of 28.00 MeV for the ^{4}He(^{3}He,p) reactions leading to the ground, 2.18-, and 3.56-MeV states in ^{6}Li. The relative standard deviations Δ are given in %, and there is an additional scale error of 1%.

^{6}Li state	Ground		2.18 MeV		3.56 MeV	
θ_{lab} (deg)	$\sigma_{c.m.}$ (mb/sr)	Δ (%)	$\sigma_{c.m.}$ (mb/sr)	Δ (%)	$\sigma_{c.m.}$ (mb/sr)	Δ (%)
15	4.40	3.0	20.9	1.4	0.40	10
20	3.12	2.4	16.6	3.6	0.32	16
25	2.36	5.5	12.6	4.0	0.38	21
30	2.20	7.7	9.23	3.1	0.46	13
35	2.09	3.3	7.30	1.9	0.66	8
40	2.28	3.2	6.05	2.1	0.61	10
45	2.27	3.3	5.73	2.3	0.75	8
50	2.18	3.0	5.76	2.3	0.58	12
60	2.48	3.3	5.79	2.4	0.32	16
70	2.48	3.5	4.49	2.7	0.14	29
80	2.85	3.5	3.65	3.3	...	...
90	2.85	4.6	3.14	3.8	0.29	21
100	2.40	4.6	3.08	4.2	0.24	29
110	1.82	5.5	3.64	5.5	<0.20	
120	1.79	5.0	3.91	4.1	<0.20	
130	1.73	5.2	4.26	4.0	<0.20	
140	2.32	5.2	4.36	4.4	<0.20	
150	3.02	5.0	4.25	5.2	<0.20	
160	3.50	4.9	4.50	4.7	<0.20	
165	4.15	3.4	4.37	4.1	<0.20	

drawn between the origin and the 13° data point. An uncertainty in this estimate was obtained by drawing straight lines between the origin and the error-bar tips of the 13° point. In a similar manner, an estimate of 10 ± 2 mb was obtained for the region between 45° and 54.1°. This latter angle is the largest laboratory angle at which ^{4}He continuum particles can be produced at 15.95 MeV

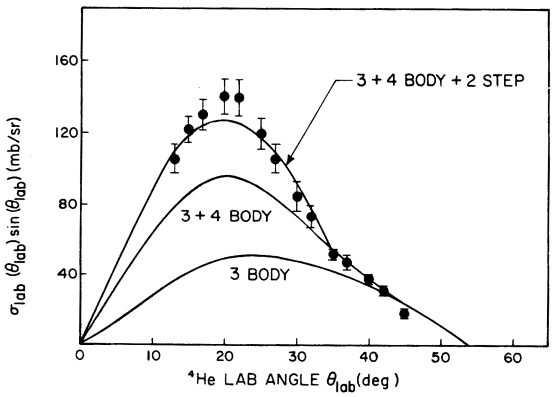

FIG. 5. Energy-integrated, ^{4}He-continuum differential cross section from the 28-MeV ^{3}He bombardment of ^{4}He. The figure shows the quantity, lab differential cross section times the sine of the lab angle, plotted vs lab angle. The solid circles show the data, and the solid curves are from the fit described in Sec. V.

(c.m.). Again, these extrapolations were in agreement with the fitting procedure discussed below in Sec. V. Addition of these two estimates to the integrated cross section obtained from the data yields an energy- and angle-integrated cross section of 398 ± 9 mb for the ^{4}He continuum.

C. Total reaction cross section

The total reaction cross section σ_R is obtained by use of Eq. (8). Addition of the cross sections for the production of ^{6}Li nuclei in the ground and second excited states to the cross section for ^{4}He continuum particles yields

$$\sigma_R = 433 \pm 10 \text{ mb}.$$

V. FIT TO THE ^{4}He CONTINUUM

The purpose of this section is to describe the fit of a simple model to the ^{4}He-continuum data. This phase of the analysis was prompted first by the occurrence of certain distinct features of the ^{4}He energy spectra which gave indications that at least two different reaction mechanisms were important, and second by the desire to have available a means having some physical content for checking the extrapolation methods described above in Sec. IV B.

A striking feature of the ^{4}He energy spectra is the occurrence of an abrupt step in all spectra mea-

sured at lab angles less than 32°. These steps are observable in Fig. 3. There the steps occur at 15 MeV in the 13° spectrum and at 10 MeV in the 27° spectrum. The energy positions of these steps agree with the calculated maximum energy a ^{4}He could have were it to be produced in the two step reaction of Eq. (3) proceeding through the first excited state of ^{6}Li. These kinematic calculations also show that this two-step reaction could not produce ^{4}He particles at lab angles greater than 34°. This is in agreement with the observed absence of the step at these larger lab angles, and it also explains the abrupt change in the slope at 34° of the energy-integrated angular distribution shown in Fig. 5. An additional characteristic of interest was that the energy position of the high-energy cutoff of the ^{4}He spectra agreed with the calculated maximum ^{4}He energy which the reaction of Eq. (1) could produce.

With this information in hand, it seemed reasonable that the detailed shape of the ^{4}He continuum might be explained by a model in which it was assumed that only the reactions of Eqs. (1) and (3) were important. When an attempt was made to fit the data under this assumption, however, the fits were poor. Therefore, the reaction of Eq. (2) was incorporated into the model to improve the fit. The final model contained the following four elements: (i) Only those reactions given in Eqs. (1), (2), and (3) are important. These reactions are, respectively, the nonsequential three-body final state reaction, the nonsequential four-body final state reaction, and the two-step sequential decay reaction which proceeds through the first excited state of ^{6}Li. (ii) For the reactions of Eqs. (1) and (2), three- and four-body phase-space functions describe the c.m. energy distribution of the ^{4}He particles. The ^{4}He continuum c.m. angular distribution for each of these reactions is described by a finite series of Legendre polynomials whose coefficients are determined by the best fit to the data. (iii) The angular distribution of the ^{6}Li* particle produced in its first excited state is obtained from our measurements of the differential cross section for the reaction ^{4}He(^{3}He, p)^{6}Li*(2.18 MeV). Therefore, in the model this angular distribution is represented by a finite series of Legendre polynomials whose coefficients are known. The angular distribution of the ^{4}He particles which come from the breakup of the excited ^{6}Li nucleus is described by a finite series of Legendre polynomials whose coefficients are determined by the best fit to the data. (iv) The model does not take into account the effects of experimental energy and angular resolution present in the ^{4}He continuum data. Further discussion of the model is given in the Appendix.

All of the ^{4}He-continuum data (approximately 1600 points) were fitted simultaneously, and the best over-all χ^2 per degree of freedom was 5.5. This fit required terms through $P_3(\cos\theta)$ in the description of the angular distribution of both the three- and four-body final state reactions and required terms only through $P_1(\cos\theta)$ in the description of the angular distribution of the ^{4}He from the ^{6}Li* in the two-step reaction. Results of this fit showed that, in the c.m. system, the angular distributions of the ^{4}He-continuum particles produced by the nonsequential decay reactions are both somewhat peaked at 180° and that the angular distribution of the ^{4}He particles produced by the decay of the ^{6}Li* is nearly uniform about the original velocity vector of the unstable ^{6}Li*.

Results of the fit at some lab angles are shown as solid curves in Fig. 3. In this figure the curves labeled "3 BODY" give the predicted energy distribution of ^{4}He particles which are produced by the reaction of Eq. (1), the curves labeled "3 + 4 BODY" give the predicted sum of the contributions from the reactions of Eqs. (1) and (2), and the curves labeled "3 + 4 BODY + 2 STEP" give the complete result, which is the sum of the contributions from the reactions of Eqs. (1)–(3). The energy-integrated angular distributions of these same curves are shown as solid curves in Fig. 5.

In Fig. 3 it is seen that the abrupt steps in the ^{4}He spectra at lab angles of 13° and 27° are closely matched by the fit, and in Fig. 5 it is seen that the abrupt change in the slope of the ^{4}He angular distribution at 34° is closely matched by the fit. It is thus clear that the cause of these abrupt changes is the onset of the two-step reaction.

Integration of the results of the fit for the individual contributions to the ^{4}He continuum gives ^{4}He production cross sections of 188 mb for the reaction of Eq. (1), 125 mb for the reaction of Eq. (2) and 81 mb for the reaction of Eq. (3). The fact that the result for the reaction of Eq. (3) agrees with the measured cross section of 81 ± 2 mb simply serves as a check on the calculation. The sum of these three contributions from the fit is 394 mb which is to be compared with the measured ^{4}He production cross section of 398 ± 9 mb.

It has been described previously how the low-energy extrapolations of the ^{4}He spectra were accomplished. The results of these extrapolations usually agreed within their estimated uncertainties with the extrapolations provided by the fit.

VI. PHASE-SHIFT STUDY

We have carried out a phase-shift study of ^{3}He + ^{4}He elastic-scattering data[14] at 15.95 MeV (c.m.) using the value of σ_R from the present experiment as an additional input datum to constrain the im-

aginary parts of the phase shifts. This study had two main purposes: (i) to ascertain whether or not least-χ^2 phase-shift solutions exist for which the real parts of the phases have values close to those of resonating-group calculations,[18] and (ii) to investigate the nature of the imaginary parts of the phases, particularly to determine to what degree they exhibit an odd-even effect, which might be correlated with a space-exchange component in the imaginary potential.[18,33]

In the phase-shift search,[34] we employed two different procedures, both of which took as starting values the resonating-group phases of Ref. 18. J splitting at this energy is expected to be small,[17,35] and none was included in the analysis. The first procedure (I) was to hold fixed initially the real parts δ_l^R of the phase shifts and to vary their imaginary parts δ_l^I until the changes in χ^2 became small. Then this new set of δ_l^I was held fixed, and the δ_l^R were varied until the changes in χ^2 again became small. This alternate variation of δ_l^R and δ_l^I was continued until a χ^2 minimum was reached. The second procedure (II) was the same as the first except that the roles of δ_l^R and δ_l^I were interchanged, with δ_l^R being varied initially. The reasoning behind the use of procedure I is that the δ_l^R of Ref. 18 are related, through the resonating-group method, to the nucleon-nucleon force, whereas the δ_l^I values of Ref. 18 are phenomenological. Therefore we attribute more physical significance to the δ_l^R than to the δ_l^I of Ref. 18, and procedure I was adopted to aid in finding solutions for which the values of δ_l^R would be close to the resonating-group values.

The present results and those of Ref. 18 are given in Table II, which lists the χ^2 and σ_R values, and in Table III, which lists the phase shifts. The fitting errors, as defined in Ref. 34, were 3 or 4 mb for σ_R and a few tenths of a degree for the phase shifts. We comment here only that Table II shows that both search procedures gave good fits, and we reserve further discussion for the next section.

TABLE II. Results for χ^2 and σ_R from fitting both the ^{3}He + ^{4}He elastic-scattering data at 15.95 MeV (c.m.) of Ref. 14 and the listed σ_R value of the present experiment. Phase-shift-search procedures I and II are described in Sec. VI.

Procedure	χ^2 per datum	σ_R (mb)
Calculation [a]	355	285 ± 40
I	0.62	446
II	0.49	432
Experiment	...	433 ± 10

[a] Resonating-group method with phenomenological imaginary potential. No attempt was made to fit the experimental value of σ_R. See Ref. 18.

VII. DISCUSSION

The fit to the ^{4}He continuum described in Sec. V verified the occurrence of the two-step reaction of Eq. (3) and the three-body breakup reaction of Eq. (1). The additional inclusion of the four-body breakup reaction of Eq. (2) was necessary in order to obtain a reasonably good fit to the data: however, in contrast to the other two reactions, no readily noticeable features were present in the continuum spectra which could be directly attributed to four-body breakup. The fit indicated that the ^{4}He yield from both the three- and four-body reactions was backward peaked with respect to the incident ^{3}He direction in the c.m. system (peripheral ^{3}He breakup) and that the total three-body yield was about 1.5 times the total four-body yield. However, considering the simplicity of the reaction model and the fact that the fit probably is not very sensitive to the detailed nature of the three- and four-body reaction modes, we feel that the conclusions concerning these modes should be taken only as rough indications. On the other hand, our fit yields the more definite result that the ^{4}He nuclei from the two-step reaction are emitted nearly isotropically in the rest system of the excited ^{6}Li nucleus. This is in contrast to the work of Ref. 26 at higher energies, where it was deduced that the ^{4}He nuclei from the two step reaction are emitted preferentially forward with respect to the ^{6}Li direction.

In Fig. 6 our measurement (solid circle) of σ_R = 433 mb for the ^{3}He + ^{4}He system at 15.95 MeV is

TABLE III. Phase shifts $\delta_l = \delta_l^R + i\delta_l^I$ in degrees for ^{3}He + ^{4}He scattering at 15.95 MeV (c.m.). Results are shown from the resonating-group calculation of Ref. 18 and from the present fit to the data of Ref. 14 along with the measured σ_R value. The two phase-shift-search procedures I and II are described in Sec. VI.

	Calculation [a]		Procedure I		Procedure II	
l	δ_l^R	δ_l^I	δ_l^R	δ_l^I	δ_l^R	δ_l^I
0	249.9	8.0	248.0	10.1	218.3	11.3
1	245.8	10.3	248.3	3.2	245.5	14.9
2	178.1	7.4	173.2	11.2	155.9	7.8
3	160.1	11.8	154.5	20.0	149.7	11.6
4	10.0	1.9	9.7	13.3	1.5	7.7
5	16.3	4.1	17.6	4.0	13.6	4.1
6	−0.4	0.1	−0.9	0.7	−3.0	3.5
7	1.3	0.1	1.0	0.4	0.1	0.3
8	−0.2	0	−0.4	0.4	−0.6	0

[a] Resonating-group method with phenomenological imaginary potential. See Ref. 18.

compared with other results. The low-energy triangle (σ_R= 135 mb at 10.2 MeV) shows the highest-energy value deduced from Ref. 4, in which complex phase-shift analyses were performed on elastic differential cross sections. It is not certain how accurate that deduced value of σ_R is; however, even in the unlikely event that it were low by as much as a factor of 2, a comparison with our value leads to the conclusion that σ_R rises rather rapidly with increasing energy in the range 10–16 MeV. The vertical bars in Fig. 6 show the σ_R results of Ref. 18, in which elastic-scattering data were fitted using the resonating-group method and a phenomenological imaginary potential. It is interesting to note that these results do show a rapid rise in σ_R over a rather narrow energy range; however, this energy region is somewhat higher than the 10–16 MeV just mentioned. It can also be seen that our measurement suggests that at 16 MeV σ_R has already attained a value near its maximum, whereas the results of Ref. 18 do not yield a leveling off of σ_R vs energy until about 21 MeV. The high-energy triangle (σ_R= 380 mb at 44 MeV) is deduced from the phase-shift analysis of Ref. 9, and that σ_R value is only about 15% below that yielded by the resonating-group analysis. We conclude from Fig. 6 that the general shape of the σ_R energy dependence yielded by the analysis of Ref. 18 is reasonable; however, that analysis predicts an energy region of rapid rise in σ_R about 5 MeV too high. We have not shown any of the optical-model results[10,11] in Fig. 6. The fits of Ref. 10 give[36] $\sigma_R > 700$ mb in the c.m. energy range 8.6–10.9 MeV; such high values clearly are unrealistic. In Ref. 11 measurements of elastic-scattering and reaction cross sections at 18 MeV (c.m.) and optical-model studies of that data are described. In that work the optical-model fits generally were required to produce large values for σ_R (>1000 mb). That requirement resulted from an unfortunate error in extracting a lower limit to σ_R from the reaction data. It has been commented elsewhere[18] that a reasonable interpretation of the data of Ref. 11 is that there is a lower limit to σ_R of 300 mb at 18 MeV, which is consistent with Fig. 6.

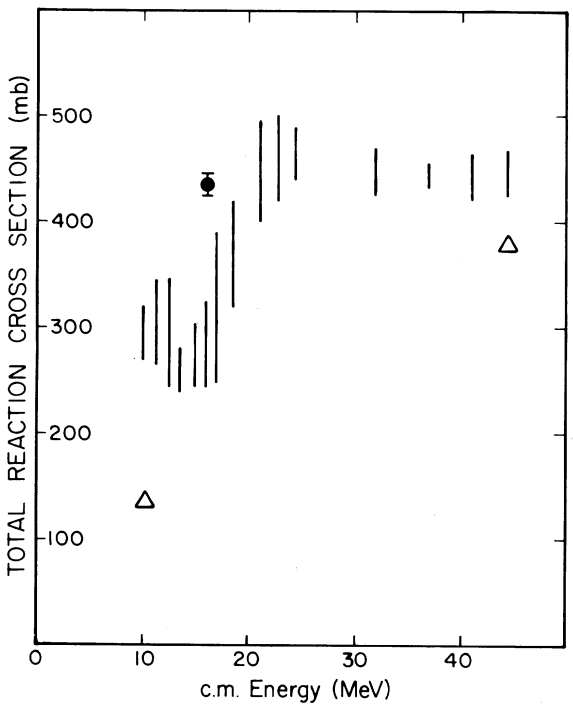

FIG. 6. Total reaction cross section vs c.m. energy for the $^3He+^4He$ system. The solid circle shows the result of the present experiment; the low-energy and high-energy triangles are from the phase-shift analyses of Refs. 4 and 9, respectively; and the vertical bars are from Ref. 18, which used the resonating-group method and a phenomenological imaginary potential.

The phase-shift study described in Sec. VI used resonating-group phase shifts[18] as starting values and had as one of its objects to see how close the fitted phases would be to the resonating-group values. There is some previous work on the study of the $^3He+^4He$ system in which this procedure was also adopted. For example, in Ref. 5 such an analysis was carried out on measurements of elastic differential cross sections in the c.m. energy range 15.5–24.4 MeV, and the phase-shift results were compared with the resonating-group calculations of Ref. 13. There the conclusion was reached that the agreement of the empirical phases with the calculated ones was rather qualitative, but that the calculated phases do provide a useful starting point for such analyses. In Ref. 9 a similar study was carried out on measurements in the c.m. energy range 28.0-44.0 MeV, and when the fitted phases were compared with the results of the resonating-group calculations described in Ref. 17, systematic differences similar to those in Ref. 5 were found to persist at these higher energies. However, a detailed comparison at 44 MeV with the resonating-group calculation of Ref. 16, which included a phenomenological imaginary potential, showed a striking similarity between the two sets of phases, particularly in the pronounced odd-even dependence on orbital angular momentum exhibited by both the real and imaginary parts of the phase shifts.

One difference between our fitting and that of Refs. 5 and 9 is that we have imposed a σ_R constraint. In addition, we have used the results of the resonating-group study of Ref. 18. This study incorporated several improvements over the calculations of Refs. 13 and 17, whose results were

used in the two investigations[5,9] just described. The main areas of improvement were the use of a nucleon-nucleon potential which fits better the low-energy two-nucleon data, the inclusion of the Coulomb-exchange terms, and the use of a phenomenological imaginary potential to account for the effects of reactions on the elastic channel. The resonating-group results at 15.95 MeV from Ref. 18 are shown in Fig. 7 as dots connected by solid lines. Also shown are the results of our fitting procedure I (dots connected by dashed lines) and fitting procedure II (dots connected by dotted lines). It can be seen in Fig. 7 that both fitting procedures yielded real phases δ_l^R which are in reasonably good agreement with the resonating-group results and that, as expected, procedure I gave δ_l^R values closer to the resonating-group values than did procedure II. It is significant that both fitting procedures yielded real phases which exhibit a marked odd-even structure in their dependence on orbital angular momentum, this dependence being quite similar to that exhibited by the resonating-group phases. This odd-even effect[37] arises in the calculations[18] from the exact treatment of the Pauli exclusion principle, and we feel that such a feature should be present in any proposed phase-shift set for this system if the set is to be considered physically realistic.

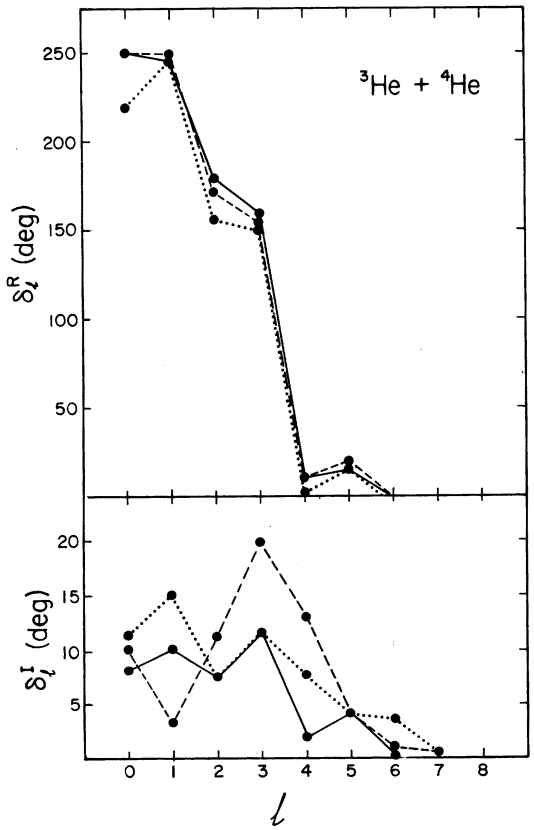

FIG. 7. Real parts δ_l^R and imaginary parts δ_l^I of the phase shifts for ^{3}He+^{4}He elastic scattering at 15.95 MeV (c.m.). The solid lines connect the results of the resonating-group study of Ref. 18, and the dashed and dotted lines connect the results of the present procedures I and II, respectively. These procedures are described in Sec. VI.

In contrast to the real phases, the imaginary phases δ_l^I display considerable variation depending on the method by which they were obtained. The odd-even nature of the dependence of δ_l^I on l shown by the resonating-group results comes from the particular form of the phenomenological imaginary potential used in Ref. 18. There, a Majorana component was included in the absorptive potential, as had been suggested from previous work,[33,38] and it was found that the experimental elastic differential cross sections were reproduced better when the absorptive strength was made larger in the odd-l than in the even-l states. Neither procedure I or II yields a structure in the l dependence of δ_l^I quite like that from Ref. 18, although, as might be expected, procedure II comes much closer to doing so than does procedure I. It appears we can conclude from this only that the present study does not establish the need for the specific type of l dependence used in the imaginary potential of Ref. 18, but rather tends to suggest that a simple odd-even dependence of the absorption may not be adequate.

Finally, we mention that we have initiated a ^{3}He + ^{4}He phase-shift study over a broad energy range using the results of Ref. 18 as starting values and have obtained some preliminary results[39] from 12 to 44 MeV (c.m.) using procedure I. The most significant result is that an odd-even effect in δ_l^R was found to exist over this full energy range.

We thank W. S. Chien and P. M Hegland for help in data taking and T. J. Woods, M. L. Halbert, F. B. Morinigo, D. R. Thompson, Y. C. Tang, and G. W. Greenlees for valuable discussions.

APPENDIX: CONTINUUM REACTION MODEL

Given here are the formulas used in and a brief discussion of the continuum model referred to in Sec. V. A detailed derivation of the formulas is presented in Ref. 29. Sequential decay also has been considered in Ref. 40.

If $\sigma(\theta,E)$ is the lab differential cross section for production of an α particle of lab energy E in the continuum at lab angle θ with respect to the incident ^{3}He direction, we calculate

$$(E'/E)^{1/2}\sigma(\theta,E)=\sigma_3(\theta',E')+\sigma_4(\theta',E') + H(\beta,\theta',E')W(\theta''), \quad \text{(A1)}$$

where (θ', E') are the α-particle angle and energy in the c.m. system corresponding to the lab quantities (θ, E), and θ'' is the angle the α particle from ^{6}Li* $\rightarrow \alpha + d$ makes in the ^{6}Li* rest system with the ^{6}Li* direction in the c.m. system. The factor $(E'/E)^{1/2}$ in Eq. (A1) is the Jacobian function for transforming the α-particle differential cross sections between the c.m. and lab systems, and the function H, which is discussed further below, transforms the ^{6}Li* breakup probability per unit solid angle $W(\theta'')$ from the ^{6}Li* rest system to the c.m. system. The cross sections σ_3 and σ_4 in Eq. (A1) describe the three- and four-body breakup processes, respectively, and are taken to be products of a phase-space energy distribution with an angular function represented by a sum of Legendre polynomials:

$$\sigma_3(\theta', E') = (E_3' - E')^{1/2}\sqrt{E'} \sum_{l=0}^{L} \lambda_l P_l(\cos\theta') , \qquad \text{(A2)}$$

and

$$\sigma_4(\theta', E') = (E_4' - E')^2\sqrt{E'} \sum_{m=0}^{M} \mu_m P_m(\cos\theta') , \qquad \text{(A3)}$$

where E_3' and E_4' are the maximum possible c.m. energies for the α particle from the appropriate decay mode. The ^{6}Li* $\rightarrow \alpha + d$ breakup probability is written as

$$W(\theta'') = \frac{1}{4\pi} + \sum_{n=1}^{N} \nu_n P_n(\cos\theta'') . \qquad \text{(A4)}$$

The derivation of the transformation function $H(\beta, \theta', E')$ in Eq. (A1) is complicated.[29] It depends on the c.m. differential cross section $\sigma_6(\theta_6')$ for the production of ^{6}Li* at c.m. angle θ_6' as well as on geometrical considerations. We write σ_6 as

$$\sigma_6(\theta_6') = \sum_{r=0}^{R} \rho_r P_r(\cos\theta_6') = \sum_{r=0}^{R} \beta_r \cos^r\theta_6' , \qquad \text{(A5)}$$

and the argument β in $H(\beta, \theta', E')$ is meant to represent the dependence of H on σ_6 through the set of coefficients β_r. We find that H can be written in the form

$$H = N_0 \sum_{r=0}^{R} \beta_r A_r(\theta', E') , \qquad \text{(A6)}$$

where N_0 depends on masses, Q values, and the incident ^{3}He energy, and can be written most simply as

$$N_0 = \left(\frac{M_6}{M_\alpha E_6' E_\alpha''}\right)^{1/2} , \qquad \text{(A7)}$$

where M_6 and M_α are the ^{6}Li and α-particle masses, respectively, E_6' is the ^{6}Li* energy in the c.m. system, and E_α'' is the α-particle energy from ^{6}Li* $\rightarrow \alpha + d$ in the ^{6}Li* rest system. The functions $A_r(\theta', E')$ in Eq. (A6) can be found from the following recursion relation

$$A_0 = \pi , \quad A_1 = \frac{\pi}{2} p ,$$

$$A_r = \frac{2r-1}{2r} p A_{r-1} + \frac{r-1}{r} q A_{r-2} , \qquad \text{(A8)}$$

where p and q are functions which can be expressed in the form

$$p = 2\cos\theta' \left[\left(\frac{E''}{E'}\right)^{1/2} \cos\theta'' + \left(\frac{M_\alpha E_6'}{M_6 E'}\right)^{1/2}\right] \qquad \text{(A9)}$$

and

$$q = \frac{E''}{E'} \sin^2\theta'' - \cos^2\theta' , \qquad \text{(A10)}$$

which allow p and q ultimately to be expressed in terms of masses, Q values, the incident ^{3}He energy, θ' and E'.

The coefficients β_r of Eq. (A5) describing the reaction ^{4}He(^{3}He, ^{6}Li*)^{1}H were obtained by fitting the data described in Sec. IV A. An upper limit of $R = 5$ to the summation was found sufficient to obtain a good fit. The coefficients λ_l, μ_m, and ν_n of Eqs. (A2), (A3), and (A4) were varied to obtain a good fit to the ^{4}He continuum data. The upper limits to the summations found necessary in these equations were $L = 3, M = 3, N = 1$, and the coefficient ν_1 of Eq. (A4) yielded by the fit was rather small.

---

*Work supported in part by the U. S. Energy Research and Development Administration.

†Present address: Los Alamos Scientific Laboratory, Los Alamos, New Mexico 87545.

[1]J. F. Dicello, G. J. Igo, and M. L. Roush, Phys. Rev. 157, 1001 (1967).

[2]J. J. H. Menet, E. E. Gross, J. Malanify, and A. Zucker, Phys. Rev. C 4, 1114 (1971).

[3]K. Wildermuth and Y. C. Tang, *A Unified Theory of the Nucleus* (Vieweg, Braunschweig, Germany, 1976).

[4]R. J. Spiger and T. A. Tombrello, Phys. Rev. 163, 964 (1967); R. J. Spiger, Ph.D. thesis, California Institute of Technology, 1966 (unpublished).

[5]P. Schwandt, B. W. Ridley, S. Hayakawa, L. Put, and J. J. Kraushaar, Phys. Lett. 30B, 30 (1969).

[6]T. A. Cahill and P. C. Martens, Bull. Am. Phys. Soc. 14, 553 (1969).

[7]A. D. Bacher, H. E. Conzett, R. de Swiniarski, H. Meiner, F. G. Resmini, and T. A. Tombrello, Bull. Am. Phys. Soc. 14, 851 (1969).

[8]W. Fetscher, K. Sattler, N. C. Schmeing, E. Seibt, Ch. Weddigen, and E. J. Kanellopoulos, Phys. Lett.

34B, 171 (1971).
[9]W. Fetscher, E. Seibt, and Ch. Weddigen, Nucl. Phys. A216, 47 (1973).
[10]F. Dunnill, T. J. Gray, H. T. Fortune, and N. R. Fletcher, Nucl. Phys. A93, 201 (1967).
[11]J. S. Vincent and E. T. Boschitz, Nucl. Phys. A143, 121 (1970).
[12]Y. C. Tang, E. Schmid, and K. Wildermuth, Phys. Rev. 131, 2631 (1963).
[13]R. E. Brown and Y. C. Tang, Phys. Rev. 176, 1235 (1968).
[14]C. G. Jacobs, Jr., and R. E. Brown, Phys. Rev. C 1, 1615 (1970).
[15]R. E. Brown, E. E. Gross, and A. van der Woude, Phys. Rev. Lett. 25, 1346 (1970).
[16]Y. C. Tang and R. E. Brown, Phys. Rev. C 4, 1979 (1971).
[17]W. Fetscher, E. Seibt, Ch. Weddigen, and E. J. Kanellopoulos, Phys. Lett. 35B, 31 (1971).
[18]J. A. Koepke, R. E. Brown, Y. C. Tang, and D. R. Thompson, Phys. Rev. C 9, 823 (1974).
[19]T. J. Gooding, Nucl. Phys. 12, 241 (1959).
[20]J. F. Dicello and G. Igo, Phys. Rev. C 2, 488 (1970).
[21]W. F. McGill, R. F. Carlson, T. H. Short, J. M. Cameron, J. R. Richardson, I. Slaus, W. T. H. van Oers, J. W. Verba, D. J. Margaziotis, and P. Doherty, Phys. Rev. C 10, 2237 (1974).
[22]R. F. Carlson, W. F. McGill, T. H. Short, J. M. Cameron, J. R. Richardson, W. T. H. van Oers, J. W. Verba, P. Doherty, and D. J. Margaziotis, Nucl. Instrum. Methods 123, 509 (1975).
[23]A. M. Sourkes, A. Houdayer, W. T. H. van Oers, R. F. Carlson, and R. E. Brown, Phys. Rev. C 13, 451 (1976).
[24]P. M. Hegland and R. E. Brown, Bull. Am. Phys. Soc. 18, 1381 (1973); John H. Williams Laboratory of Nuclear Physics Annual Report, 1976 (unpublished), p. 1.
[25]C. H. Poppe, R. E. Brown, P. M. Hegland, and J. A. Koepke, Bull. Am. Phys. Soc. 20, 578 (1975); C. H. Poppe, R. E. Brown, P. M. Hegland, J. A. Koepke, and K. Seshadri, John H. Williams Laboratory of Nuclear Physics Annual Report, 1976 (unpublished), p. 7.
[26]M. L. Halbert, A. van der Woude, and N. M. O'Fallon, Phys. Rev. C 8, 1621 (1973).
[27]P. D. Parker and R. W. Kavanagh, Phys. Rev. 131, 2578 (1963).
[28]F. Ajzenberg-Selove and T. Lauritsen, Nucl. Phys. A227, 1 (1974).
[29]J. A. Koepke, M.S. thesis, University of Minnesota, 1975 (unpublished).
[30]W. S. Chien, Ph.D. thesis, University of Minnesota, 1974 (unpublished).
[31]W. S. Chien and R. E. Brown, Phys. Rev. C 10, 1767 (1974).
[32]Type-H polyimide film, Du Pont, Wilmington, Delaware 19898.
[33]D. R. Thompson, Y. C. Tang, and R. E. Brown, Phys. Rev. C 5, 1939 (1972).
[34]The searching technique was the "square matrix search" method of R. A. Arndt and M. H. MacGregor, in *Methods in Computational Physics*, edited by B. Alder, S. Fernbach, and M. Rotenberg (Academic, New York, 1966), Vol. 6, p. 253.
[35]R. D. Furber, Ph.D. thesis, University of Minnesota, 1976 (unpublished).
[36]No σ_R values were listed in Ref. 10. We have calculated them from the potential parameters in Table I of that reference.
[37]R. E. Brown, F. S. Chwieroth, Y. C. Tang, and D. R. Thompson, Nucl. Phys. A230, 189 (1974), and references therein.
[38]D. R. Thompson, Y. C. Tang, J. A. Koepke, and R. E. Brown, Nucl. Phys. A201, 301 (1973).
[39]J. A. Koepke and R. E. Brown, John H. Williams Laboratory of Nuclear Physics Annual Report, 1976 (unpublished), p. 13.
[40]F. B. Morinigo, Nucl. Phys. A127, 116 (1969). We do not agree with the results of this reference, in which there are apparently some typographical errors. For instance, the expression for a in Eq. (30) of this reference does not follow from the line immediately preceding it. Communications with the author have not yet fully resolved the disagreement.